Naval Surface Warfare Center
Carderock Division
West Bethesda, MD 20817-5700

NSWCCD-50-TR–2002/061 December 2002

Hydromechanics Directorate

Technical Report

Flow Predictions for Multi-Element Control Surfaces

by

Yu-Tai Lee

Michael P. Ebert

Ashvin Hosangadi

NSWCCD-50-TR–2002/061

REPORT DOCUMENTATION PAGE

Form Approved
OMB No. 0704-0188

1. REPORT DATE *(DD-MM-YYYY)*	2. REPORT TYPE	3. DATES COVERED *(From - To)*
20-Dec-2002	Final	1-Jan-2000 - 30-Sept-2001

4. TITLE AND SUBTITLE
Flow Predictions for Multi-Element Control Surfaces

5a. CONTRACT NUMBER

5b. GRANT NUMBER

5c. PROGRAM ELEMENT NUMBER

6. AUTHOR(S)
Y. T. Lee, M. P. Ebert and A. Hosangadi

5d. PROJECT NUMBER
93R1-01-HY

5e. TASK NUMBER
HY-01-DI-1

5f. WORK UNIT NUMBER
1-5050-107

7. PERFORMING ORGANIZATION NAME(S) AND ADDRESS(ES) AND ADDRESS(ES)
Naval Surface Warfare Center
Carderock Division
9500 Macarthur Boulevard
West Bethesda, MD 20817-5700

8. PERFORMING ORGANIZATION REPORT NUMBER
NSWCCD-50-TR-2002/061

9. SPONSORING / MONITORING AGENCY NAME(S) AND ADDRESS(ES)
Attn SEA 93R
Commander
Naval Sea Systems Command
2531 Jefferson Davis Highway
Arlington, VA 22242-5160

10. SPONSOR/MONITOR'S ACRONYM(S)

11. SPONSOR/MONITOR'S REPORT NUMBER(S)

12. DISTRIBUTION / AVAILABILITY STATEMENT
Distribution is unlimited. Requests for this document shall be referred to the Naval Surface Warfare Center, Carderock Division, Code 5400.

13. SUPPLEMENTARY NOTES

14. ABSTRACT
The TAC (Tab-Assisted Control) and FlexTAC (Flexible Tab-Assisted Control) airfoils based on NACA 0018 sections are conceptual multi-element airfoil designs for future marine vehicle control surfaces. In addition to a relative motion between the stabilizer and the flap, either a rigid (for TAC) or a flexible (for FlexTAC) tab is used to augument the functionality of the control surfaces. The TAC airfoil has a front and a rear gap while FlexTAC airfoil has only the front gap. This report summarizes CFD validations on the TAC and FlexTAC airfoils using unstructured Reynolds Averaged Navier Stokes (RANS) solvers, i.e. UNCLE and CRUNCH codes. The force and moment predictions are compared with the 24-inch water-tunnel test data obtained for the TAC airfoil and the 36-inch water-tunnel data obtained for the FlexTAC airfoil. The CFD results suggest that the UNCLE and CRUNCH codes are able to predict the forces and moments with reaonaobe accuracy for flap angles under 20 degrees. The comparisons also indicate that the FlexTAC measured force data may have been over-corrected for the water-tunnel blockage. Comparisons between the measured TAC data and FlexTAC data imply that the gudgeons installed for the TAC experiments have a profound effect on the stabilizer and flap torque calculations, but have a minimum effect on the force calculations. The CFD prediction results also indicate that ..

15. SUBJECT TERMS
Multi-Element Airfoil, Computational Fluid Dynamics, Reynolds Averaged Navier Stocks, Tab Assisted Control, Flexible Tab Assisted Control

16. SECURITY CLASSIFICATION OF:			17. LIMITATION OF ABSTRACT	18. NUMBER OF PAGES	19a. NAME OF RESPONSIBLE PERSON
a. REPORT	b. ABSTRACT	c. THIS PAGE			Yu-Tai Lee
UNCLASSIFIED	UNCLASSIFIED	UNCLASSIFIED	SAR	0	19b. TELEPHONE NUMBER *(include area code)* 301-227-1328

THIS PAGE INTENTIONALLY LEFT BLANK

Contents

Figures

Tables

Abstract

The TAC (Tab-Assisted Control) and FlexTAC (Flexible Tab-Assisted Control) airfoils based on NACA 0018 sections are conceptual multi-element airfoil designs for future marine vehicle control surfaces. In addition to a relative motion between the stabilizer and the flap, either a rigid (for TAC) or a flexible (for FlexTAC) tab is used to augment the functionality of the control surfaces. The TAC airfoil has a front and a rear gap while FlexTAC airfoil has only the front gap. This report summarizes CFD validations on the TAC and FlexTAC airfoils using unstructured Reynolds Averaged Navier Stokes (RANS) solvers, i.e. UNCLE and CRUNCH codes. The force and moment predictions are compared with the 24-inch water-tunnel test data obtained for the TAC airfoil and the 36-inch water-tunnel data obtained for the FlexTAC airfoil. The CFD results suggest that both UNCLE and CRUNCH codes are able to predict the forces and moments with reasonable accuracy for flap angles under 20 degrees. The comparisons also indicate that the FlexTAC measured force data may have been over-corrected for the water-tunnel blockage. Comparisons between the measured TAC data and FlexTAC data imply that the gudgeons installed for the TAC experiments have a profound effect on the stabilizer and flap torque predictions, but have a minimum effect on the force predictions. The CFD prediction results also indicate that it is essential to include the gap effect in calculating forces and moments.

Administrative Information

The work described in this report was performed by the Propulsion and Fluid Systems Department (Code 5400) of the Hydromechanics Directorate at the Naval Surface Warfare Center, Carderock Division (NSWCCD) and CRAFT Tech, Inc. The work was funded by the Naval Sea Systems Command (NAVSEA), Advanced Submarine Technology Office, 93R as part of the Flexible Tab-Assisted Control Task of the 6.4 Maneuvering and Control R&D Program under work unit number is 1-5050-107.

Acknowledgements

Computer resources for the computations described in this report were provided by the Army Engineer Research and Development Center (ERDC) Major Shared Resource Center through the DoD High Performance Computing Modernization Program. Additional computer resources were provided by the United States Navy's Hydrodynamics and Hydroacoustics Technology Center located at NSWCCD. The test data for the TAC and FlexTAC experiments were obtained from Scott Gowing. Kirk Anderson performed the flow visualization for the FlexTAC airfoil in the 36-inch water tunnel. C. H. Sung provided the TAC geometry through one of his early CFD grids.

Introduction

The tab assisted control (TAC) airfoil for underwater control surfaces was tested in the 24-inch water tunnel at NSWCCD during 1998 under ONR and DARPA funding. Results (Nguyen

et al., 1999) indicated that the addition of a tab to regular control surfaces can enhance the maneuvering capabilities through significant modification of lift and torque on the control surfaces.

The benefit of the TAC concept can be further augmented by using Shape Memory Alloy (SMA) actuators and shape optimization for the complete control surfaces. Employing SMA actuators enables the use of electric power to manipulate the control surfaces, and eliminates the need for hydraulic systems and the gap between the flap and the tab. These advantages led to the development of the flexible tab assisted control (FlexTAC) surfaces for underwater vehicle applications. The optimization effort under the current NAVSEA 93R FlexTAC Program aims to numerically achieve optimal sternplane designs for future FlexTAC surface applications.

Sung and Rhee (1999) and Sung et al. (2000) used a CFD tool to predict forces and moments on the TAC airfoil. The agreement with the measured data seems to be good. But the comparisons are restricted to the linear portion of the data. Although there are three possible relative angular settings between the stabilizer, the flap and the tab, the numerical investigations (Sung et al., 2000) are only limited to one angular motion for each comparison. In addition, the effect of the gaps between the stabilizer and the flap and between the flap and the tab was neglected in Sung and Rhee (1999) and not addressed in Sung et al. (2000). In fact, the TAC airfoil shown in Fig. 1 and used for the 24-inch water-tunnel test (Nguyen et al., 1999) contains (1) a pedestal to minimize the tunnel boundary-layer effect on the measured forces and moments; and (2) gudgeons to connect the stabilizer, the flap and the tab, and to control their relative motions. These gudgeons also affect the gap flow fields. The FlexTAC airfoil experiment (Gowing, 2002) conducted during March 2002 in the 36-inch water tunnel does not have the pedestal and gudgeons. However, the stabilizer for the latter experiment was installed with a turbulent-flow stimulator near the foil's leading edge. The dimensions normalized by the mid-chord length of 19.791 inches for the FlexTAC airfoil, compared with the mid-chord length of 9.526 inches for the TAC airfoil, are shown in Fig. 2.

A Direct Method for Optimization (DMO) (Lee et al., 2001) was recently developed and used for achieving an optimal diffuser shape for a shipboard air-conditioning compressor. The mathematical requirement of an optimization scheme is to maximize (or minimize) an objective (or an output) function, which represents the parameter of interest from a mathematical model of the problem. The DMO developed is a gradient-based approach coupled with a CFD calculation and a regridding approach to iteratively march to an optimal shape. The CFD method used for the diffuser optimization is a structured-grid calculation scheme. The proposed DMO for the control surface shape optimization is to adopt an unstructured CFD scheme to accommodate the gap geometry and grid movement requirements. The objective function for future control surface optimization will be a composite function of lift and torque calculated.

The goal for the current efforts is twofold. The initial goal is to carefully validate the prediction ability of unstructured CFD calculations for the TAC and FlexTAC airfoils. The ultimate goal is to use the numerical optimization procedure to achieve control surface shapes, which provide better maneuvering capabilities under given maneuvering requirements.

Computational Schemes and Grids

Two computational approaches were used to investigate the predictive capabilities for the FlexTAC and the TAC airfoils. Both approaches perform RANS calculations on a

computational domain extending 2 chord lengths upstream and 4.5 chords downstream of the airfoil, 3 chord lengths in the transverse direction, and 2 chord lengths in the spanwise direction.

The first RANS approach uses the unstructured UNCLE code (Hyams et al., 2002). UNCLE solves the incompressible Navier Stokes equations with the artificial compressibility. The flow solver is a node-centered, finite volume, implicit time-marching scheme. The flow variables are stored at the vertices. A one-to-one mapping is used to convert the edge information to the faces of the control volumes. UNCLE is programmed for parallel processing, using MPI for interprocessor communication and a coarse-grained domain decomposition for concurrent solution within subdomains assigned to multiple processors. A two-equation q-ω turbulence model (Coakley and Hsieh, 1985) is used for the present work.

The grids used for the UNCLE calculations are multi-element unstructured grids generated using an advancing normal methodology for the boundary layer elements and an advancing front/local reconnection (AFLR) methodology (Marcum and Weatherill, 1994) for the isotropic tetrahedral elements. Surface grid generation and geometry preparation were accomplished using SolidMesh (Gaither et al., 2000). Special attention was paid to the grid spacing in the gaps between the stabilizer, the flap and the tab to avoid poor grid quality. The gudgeons are not modeled in these calculations, resulting in airfoil elements that are completely disconnected from each other. A symmetry boundary condition is applied on the plane formed by the root section of the airfoil and a far-field boundary condition is employed at a sufficient distance away from the wing to avoid any influence on the solution. The surface grids on the symmetry plane and the airfoil are shown in Fig. 3. The total number of cells for each grid is around 3.5 million.

The second RANS approach uses the unstructured CRUNCH code (Hosangadi et al., 1996; Ahuja et al., 2001) developed by CRAFT Tech, Inc. The CRUNCH code solves multiphase incompressible and compressible gas-liquid Navier Stokes equations. The solver uses a finite-volume Roe/TVD flux construction based on the cell-vertex formulation. The numerical integration uses explicit four-stage Runge-Kutta, implicit GMRES, and Gauss-Seidel schemes. The code works for multi-element grids including tetrahedral, hexahedral, prismatic and pyramid cells. CRUNCH is programmed for parallel processing, using MPI and an automated load balancing domain decomposition. A dynamic grid capability, which is essential for future optimization of the control surfaces, using a node movement solver is available for automated embedding and sliding interfaces. A two-equation k-ε turbulence model with a wall function approach is used for the current calculations.

The grids used for the CRUNCH calculations are generated using GRIDGEN. They consist of hexahedral grids with approximately 2.5 million cells. The pedestal and the gudgeons are not modeled. The outer domains are treated with far-field boundary conditions. The airfoil root surface is treated as an inviscid wall due to the use of the pedestal for the TAC experiment.

Flow Conditions and Computational Strategy

The simulations under the current effort include both TAC and FlexTAC airfoils.

For the TAC airfoil, the tip chord is 8.40 inches, the root chord 10.66 inches, and the span 8.44 inches. Both the flap and tab gaps are 1/16 inch with the flap gap widened at both ends. The computational grid is non-dimensionalized by the (mean) chord length at mid span, which is 9.526 inches. Based on this dimension and the nominal test speed of 11.13 ft/s the Reynolds

number for the flow is 9.7×10^5. Hinge points for torque calculations are located at x = 0.3085 for the stabilizer, x = 0.8011 for the flap, and x = 1.0186 for the tab in non-dimensional units. Note that the experimentally installed pedestal and the gudgeons are not modeled, as mentioned in the previous sections. The deflection angles for the stabilizer (α), the flap (δ_F) and the tab (δ_T) are measured with respect to the incoming flow, the stabilizer and the flap, respectively. The measured ranges of α, δ_F, and δ_T are from –15 to 15 degrees, from –27 to 27 degrees, and from –60 to 60 degrees, respectively.

For the FlexTAC airfoil, the dimensions are normalized by the mid-span chord of 19.791 inches (see Fig. 2). The pre-test calculations were performed at a nominal speed of 10 ft/s and a Reynolds number of 1.833×10^6. The test was later performed at a lower speed of 8.5 ft/s due to limitations of the SMA materials.

Since the initial CFD validation for the TAC airfoil by Sung et al. (2000) used structured grids, the current effort does not intend to duplicate the previous calculations. The current approach of using an unstructured grid methodology aims to achieve gridding flexibility in the gap region and also to enable grid movement for future airfoil shape modification during automated numerical optimization. Three flow cases are used to validate the abilities of UNCLE and CRUNCH to predict general flow features and the gap effect. These three cases are:

Case A: $\alpha = 0$, $\delta_T = 0$, δ_F varying between –27 and 27 degrees

Case B: $\alpha = 6$, $\delta_T = 0$, δ_F varying between –27 and 27 degrees

Case C: $\alpha = 0$, $\delta_F = 10$, δ_T varying between –60 and 60 degrees

All three cases are within the normal range of the control-surface operation. Case A is the baseline case with relative motion only between the stabilizer and the flap. Case B is similar to Case A, but the stabilizer is under an angle of attack. Case C provides the validation for changing the tab angle. Due to limitations of time and funding resources, CFD validations using the UNCLE and CRUNCH codes were not conducted for all the cases mentioned. Table 1 lists the measured data used for comparison. Tables 2 and 3 show the cases predicted by the CRUNCH and UNCLE codes, respectively. For the pre-test predictions on the FlexTAC airfoil, only Case B with δ_F = -20, 0, 10, and 20 deg. were calculated.

Computational Results for the TAC Airfoil

The 24-inch water-tunnel measurements (Nguyen et al., 1999) for the TAC airfoil include overall lift and drag on the airfoil and torques acting on the stabilizer, the flap with the tab, and the tab. These measured quantities are compared to the predictions in a non-dimensional form based on the chord length at mid-span (c_m). They include lift and drag coefficients (normalized by $\frac{1}{2} \rho V_\infty^2 c_m^2$) and stabilizer, flap and tab torque coefficients (normalized by $\frac{1}{2} \rho V_\infty^2 c_m^3$).

Figures 4 – 6 show the comparisons between the measured and the predicted data for Cases A and B. For Case A (circle symbols), the computations preserve the symmetry between the positive and the negative flap angles. The measured data show some deviations from symmetry, particularly in the drag curve with a difference of 11% for the flap angles of ±27 degrees. At zero δ_F (the case used for a quantitative evaluation of the drag prediction), UNCLE predicts 63% more drag than the measurement and CRUNCH predicts 83% more. This is due to the fact that flow transition from laminar to turbulent flow occurs in the experiment while the CRUNCH

prediction assumes a fully turbulent flow over the entire airfoil and the UNCLE prediction based on the q-ω turbulence model contains some transition effect. For Case B (triangle symbols), the lift values shown in Fig. 4 are greater than those from Case A due to the positive angle of attack for the stabilizer. This also produces asymmetry in the drag curves, shifting them to the left as shown in Fig. 4. Although CRUNCH does a slightly better job, both UNCLE and CRUNCH predict the forces reasonably well except for flap angles larger than 20 degrees. For the torque predictions on the stabilizer and the combined flap and tab, the predicted trends are quite different from the measured ones. The predicted tab torque, however, agrees very well with the measurement. Note that the stabilizer torque is of the same order of magnitude as the flap torque and it is an order of magnitude larger than the tab torque. All of these observations suggest that the discrepancy in predicting stabilizer and flap torques is not directly associated with the prediction accuracy. Further comparisons between the measurements of the TAC and FlexTAC airfoils indicate that the discrepancy is mostly related to the difference in the gap flows.

Figure 7 shows similar comparisons for Case C, which maintains a fixed relative angle between the stabilizer and the flap and varies the tab angles. Similarly, the lift and drag forces are predicted well for smaller tab angles. Although the stabilizer and flap torques are over-predicted, the trends in torque predictions agree with the measurements. Again, the tab torques are predicted very well even though their values are an order of magnitude smaller than those for the stabilizer and the flap.

Figure 8 shows the pressure distributions for Case A at the positive flap angles. They clearly indicate that flow separates on the suction side between 10 and 15 degrees flap angle. Vortices shed from the pressure-side trailing corner of the stabilizer (shown in Fig. 9) fill the gap void for larger flap angles and move the pressure-side peak on the flap pressure distribution further downstream due to an increase in size of the gap region. They also provide feedback to the trailing corner area of the stabilizer. All these phenomena indicate that the front gap between the stabilizer and the flap has a dramatic effect on the local flow field, particularly near the leading edge of the flap (which has the pressure peak on the pressure side) and the trailing corner of the stabilizer. Since the tab angle is fixed at zero for Case A, the rear gap effect is not as pronounced as the front gap.

Computational Results for the FlexTAC Airfoil

The 36-inch water tunnel tests (Gowing, 2002) for the FlexTAC airfoil measured similar quantities as for the TAC airfoil. Since the profile shapes of the flexible portion of the FlexTAC airfoil were not known beforehand, the pre-tested predictions were done assuming it to be rigid. In addition, the limited calculations were focused on settings similar to those of Case B.

The comparisons are plotted in Figs. 10 and 11 along with the Case B TAC results. Note that blue symbols are used for the TAC airfoil data and red symbols for the FlexTAC airfoil data. The measured FlexTAC lift and drag are lower than the measured TAC values, particularly for flap angles less than 0 deg. and greater than 18 deg. The predicted FlexTAC lift and drag values are generally higher than the measured values. This suggests that the measured FlexTAC forces may have been over-corrected for the water-tunnel blockage effect. Although the blockage correction is perhaps too large, the measured FlexTAC drag at $\alpha = \delta_F = \delta_T = 0$ is 0.0162, which is 35 % higher than the measured TAC drag of 0.01202. This is obviously the contribution of the turbulent stimulator installed in the FlexTAC experiments. Figure 11 shows the stabilizer and

flap torque comparisons. There is a clearly different trend between the FlexTAC and the TAC airfoils. The CFD predictions have predicted the trend of the FlexTAC experiments correctly. The effects of the gap flow and the gudgeons on the torque calculations are obvious from the differences between the two measured data sets and the CFD predictions.

A flow visualization at $\alpha = 6$ deg., $\delta_F = 10$ deg., and $\delta_T = 0$ deg. was also made for the FlexTAC airfoil to further validate the CFD predictions in the airfoil tip region. Figure 12 shows pressure side paint traces compared to predicted particle traces on the pressure side surface. The three paint trace photos gradually zoom in to the flap portion in order to see the detailed streamline pattern. The installation of the sand-grain turbulent stimulator is clearly shown on the stabilizer. The tip flow from the pressure side to the suction side is also demonstrated on both traces. The stagnation line at the leading edge of the flap is shown in the prediction, but not illustrated in the experiment due to the high viscosity of the paint. Figure 13 shows a similar comparison on the suction side, but the flow is from right to left. Again, the paint on the stabilizer (orange) was too thick to show any movement. In addition, the flap at the tip was not aligned well with the stabilizer and its leading edge protruded out by about 1/16 inch. It therefore produced an unrealistic streakline that sweeps down from the flap nose to the SMA (green) area. Otherwise the paint traces agree well with the flow particle traces. Figure 14 shows the flow feature over the tip cap of the stabilizer. Both the experimental paint and the predicted streamline traces agree well. The paint over the flap tip was too thick to show any traces and therefore omitted.

Concluding Remarks

The TAC and FlexTAC airfoils based on NACA 0018 sections are conceptual designs for future marine vehicle control surfaces. In addition to relative motion between the flap and the stabilizer, either a rigid (TAC) or a flexible (FlexTAC) tab is used to augment the functionality of the control surface. The TAC airfoil has a front and a rear gap while the FlexTAC airfoil has only the front gap. This report summarizes CFD validations on the TAC and FlexTAC airfoils using the unstructured UNCLE and CRUNCH RANS codes. The force and moment predictions are compared with the 24-inch water-tunnel test data for the TAC airfoil and the 36-inch water-tunnel data for the FlexTAC airfoil. The following conclusions are drawn from the validation calculations.

(1) Both the UNCLE and CRUNCH codes are able to predict the forces and moments with reasonable accuracy for flap angles smaller than 20 deg. Although both predictions deviate from the measured data for flap angles greater than 20 deg., CRUNCH predicts more accurate forces while UNCLE predicts more accurate moments.

(2) At zero deflection for stabilizer, flap and tab, the measured drag on the TAC foil is 0.01202, which is 63 – 83 % lower than the predictions. This is due to the existence of flow transition in the test but not in the calculations. Although there is a turbulent stimulator installed in the FlexTAC experiment, the measured drag of 0.0162 is only 35 % higher than that of the TAC experiment. The overall FlexTAC measured data indicate that the forces may have been over-corrected for the water tunnel blockage.

(3) The comparisons between the measured TAC and FlexTAC data suggest that the gudgeons have a profound effect on the stabilizer and flap torque calculations, but have a minimum effect on the force calculations.

(4) The CFD predictions further emphasizes the importance of the gap effect on the forces and moments.

THIS PAGE INTENTIONALLY LEFT BLANK

	alpha	delFlap	delTab	EXP	Drag	Lift	Stab_Torq	Flap_Torq	Tab_Torq
CaseA	0	-27	0	x	0.149769	-0.49547	0.0173029	0.009977	0.001096
	0	-20	0	x	0.095064	-0.4172	0.0157057	0.005286	0.00066
	0	-10	0	x	0.03707	-0.22228	0.0090129	0.001331	0.000183
	0	0	0	x	0.01202	-0.00237	-0.00025	-0.0001	0.00001
	0	10	0	x	0.032975	0.225015	-0.0102283	-0.00199	-0.00016
	0	20	0	x	0.085103	0.416893	-0.0155871	-0.00615	-0.00063
	0	27	0	x	0.132977	0.481604	-0.0175886	-0.00966	-0.00098
CaseB	6	-27	0	x	0.096797	-0.27833	0.0237471	0.006136	0.000894
	6	-20	0	x	0.057829	-0.19139	0.0211714	0.00313	0.000454
	6	-10	0	x	0.023804	-0.00019	0.01694	0.000569	0.000129
	6	0	0	x	0.022334	0.237714	0.0026006	0.00101	0.000126
	6	10	0	x	0.070027	0.455027	-0.0027057	-0.00385	-0.00029
	6	20	0	x	0.14063	0.59999	-0.0066514	-0.00966	-0.00111
	6	27	0	x	0.196059	0.6618	-0.00722	-0.01383	-0.00111
CaseC	0	10	-60	x	0.053285	0.021875	-0.005325	0.01811	0.002935
	0	10	-40	x	0.03855	0.09085	-0.0075	0.01384	0.0018
	0	10	-20	x	0.02847	0.15165	-0.00896	0.00751	0.00059
	0	10	0	x	0.032975	0.225015	-0.0102283	-0.00199	-0.00016
	0	10	20	x	0.06261	0.37045	-0.01369	-0.01698	-0.00152
	0	10	40	x	0.10385	0.48572	-0.0171	-0.02684	-0.00306
	0	10	60	x	0.134445	0.5408	-0.019005	-0.02867	-0.00405

Table 1. Measured forces and moments for the TAC airfoil from 24-inch water tunnel test.

	alpha	delFlap	delTab	CRUNCH	Drag	Lift	Stab Torq	Flap Torq	Tab Torq
CaseA	0	-27	0	x	0.131478	-0.375244	0.002274	0.007498	0.000804
	0	-20	0	x	0.085917	-0.361595	0.005265	0.000727	0.000439
	0	-10	0	x	0.039462	-0.237148	0.005674	-0.003057	0.000014
	0	0	0	x	0.021969	-0.002084	-0.001511	-0.000232	-0.000003
	0	10	0	x	0.039462	0.237148	-0.005674	0.003057	-0.000014
	0	20	0	x	0.085917	0.361595	-0.005265	-0.000727	-0.000439
	0	27	0	x	0.131478	0.375244	-0.002274	-0.007498	-0.000804
CaseB	6	-27	0						
	6	-20	0						
	6	-10	0						
	6	0	0						
	6	10	0	x	0.073554	0.4562804	0.000234	0.002668	-0.000077
	6	20	0	x	0.133398	0.555350	0.001670	-0.003757	-0.000568
	6	27	0	x	0.186796	0.604788	0.002639	-0.009502	-0.000955
CaseC	0	10	-60						
	0	10	-40	x	0.039864	-0.037518	-0.001880	0.023875	0.001900
	0	10	-20						
	0	10	0	x	0.039462	0.237148	-0.005674	0.003057	-0.000014
	0	10	20						
	0	10	40	x	0.122600	0.585600	-0.010959	-0.024500	-0.003283
	0	10	60						

Table 2. Predicted forces and moments for the TAC airfoil by CRUNCH

	alpha	delFlap	delTab	UNCLE	Drag	Lift	Stab_Torq	Flap_Torq	Tab_Torq
CaseA	0	-27	0	x	0.1199	-0.3023	-0.0004	0.0113	0.0009
	0	-20	0	x	0.0850	-0.3208	0.0034	0.0049	0.0007
	0	-10	0	x	0.0326	-0.2208	0.0051	-0.0033	0.0001
	0	0	0	x	0.0196	-0.0004	0.0001	0.0000	0.0000
	0	10	0	x	0.0326	0.2208	-0.0051	0.0033	-0.0001
	0	20	0	x	0.0850	0.3208	-0.0034	-0.0049	-0.0007
	0	27	0	x	0.1199	0.3023	0.0004	-0.0113	-0.0009
CaseB	6	-27	0	x	0.0966	-0.1053	0.0051	0.0094	0.0008
	6	-20	0	x	0.0416	-0.2089	0.0137	-0.0066	0.0003
	6	-10	0	x	0.0225	0.0175	0.0119	-0.0028	0.0001
	6	0	0	x	0.0296	0.2021	0.0144	0.0013	0.0001
	6	10	0	x	0.0638	0.4245	0.0019	0.0025	-0.0002
	6	20	0	x	0.1233	0.4805	0.0046	-0.0087	-0.0008
	6	27	0	x	0.1641	0.5058	0.0064	-0.0137	-0.0010
CaseC	0	10	-60						
	0	10	-40						
	0	10	-20						
	0	10	0	x	0.0326	0.2208	-0.0051	0.0033	-0.0001
	0	10	20						
	0	10	40						
	0	10	60						

Table 3. Predicted forces and moments for the TAC airfoil by UNCLE

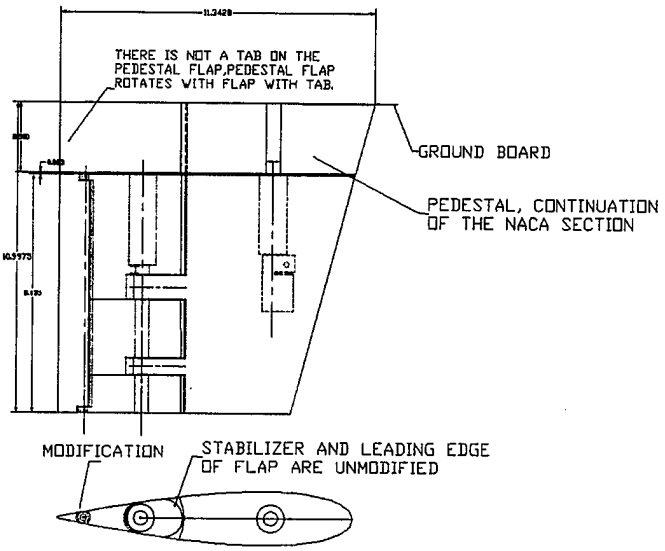

Figure 1. Schematics for the 24-inch water-tunnel test on the TAC airfoil.

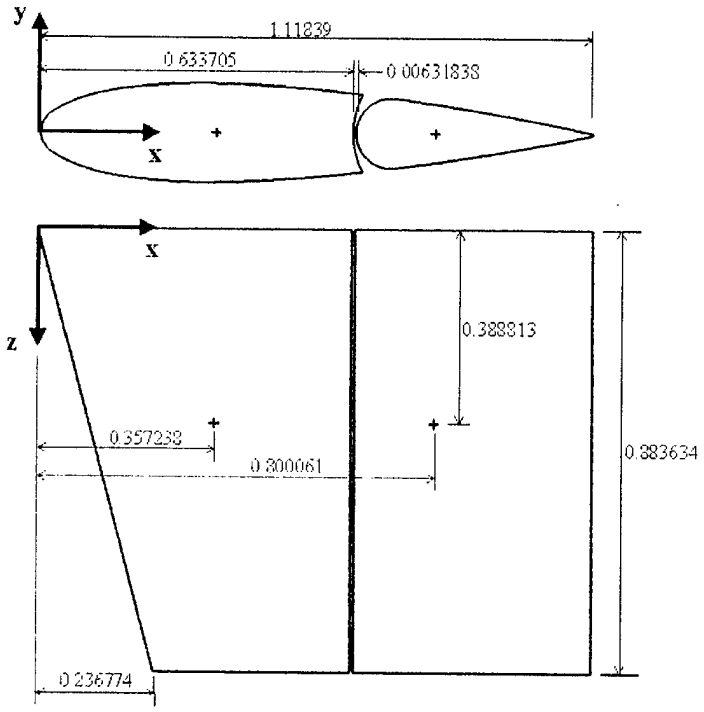

Figure 2. The FlexTAC airfoil for the 36-inch water tunnel test (all dimensions are normalized by the mid-span chord of 19.791 inches).

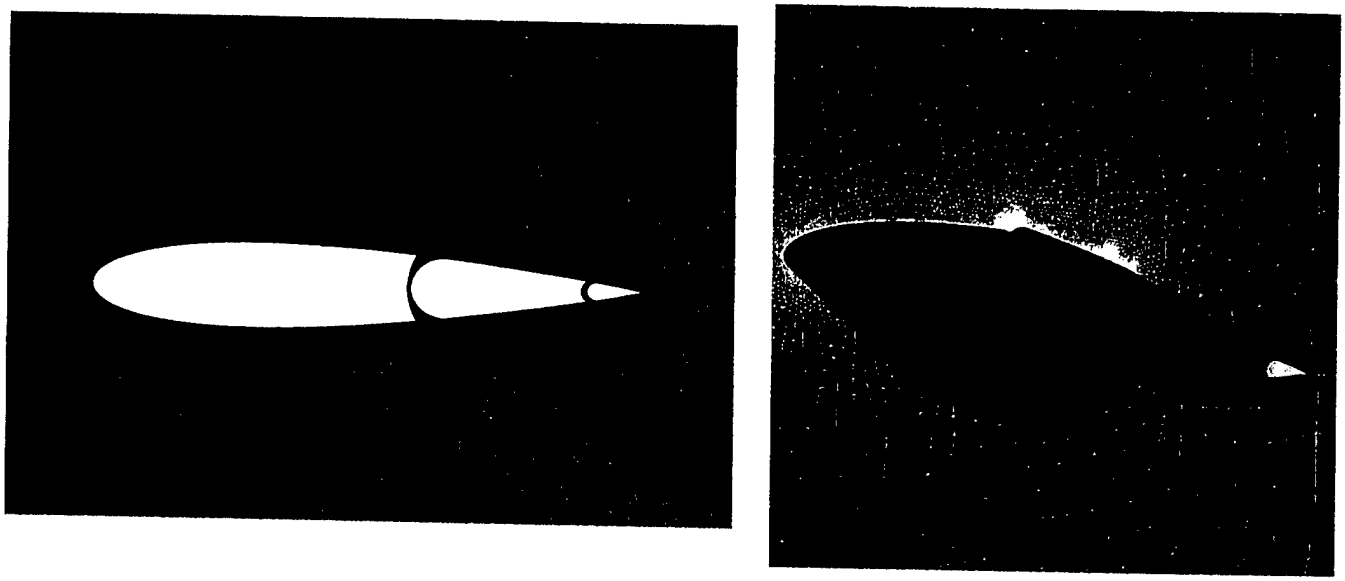

Figure 3. Unstructured grid for the TAC airfoil.

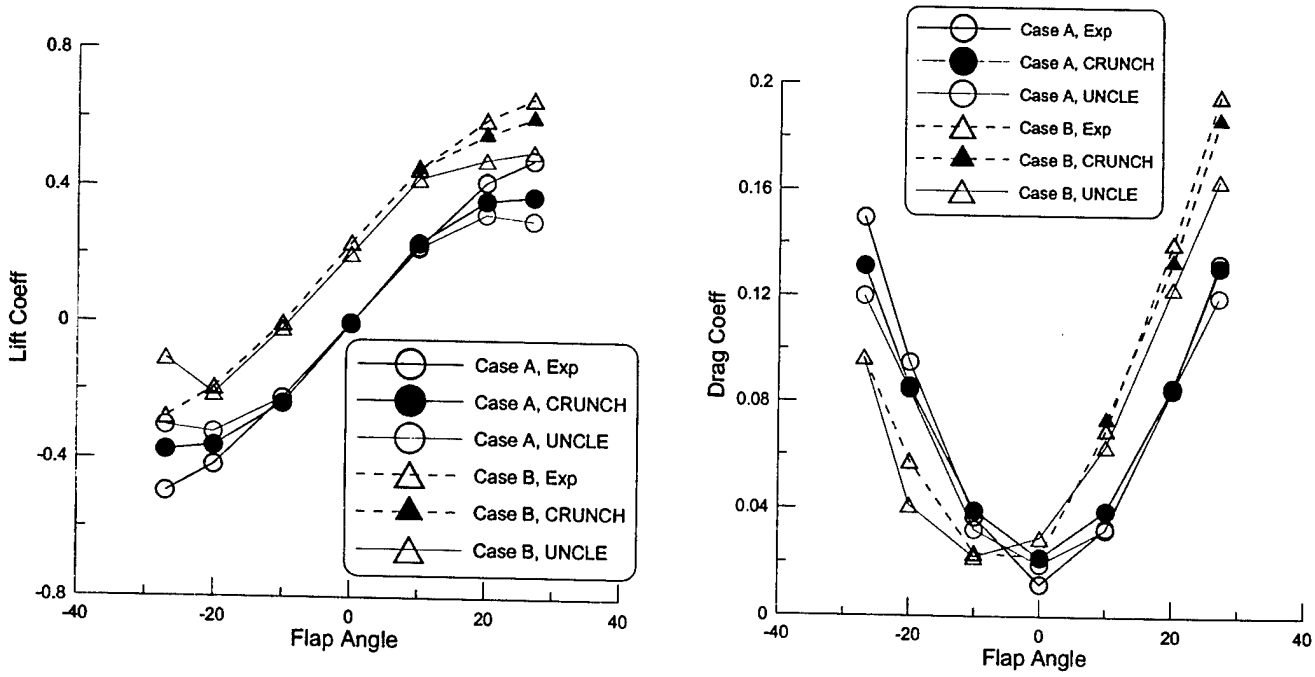

Figure 4. Lift and drag comparisons on TAC airfoil for Cases A and B.

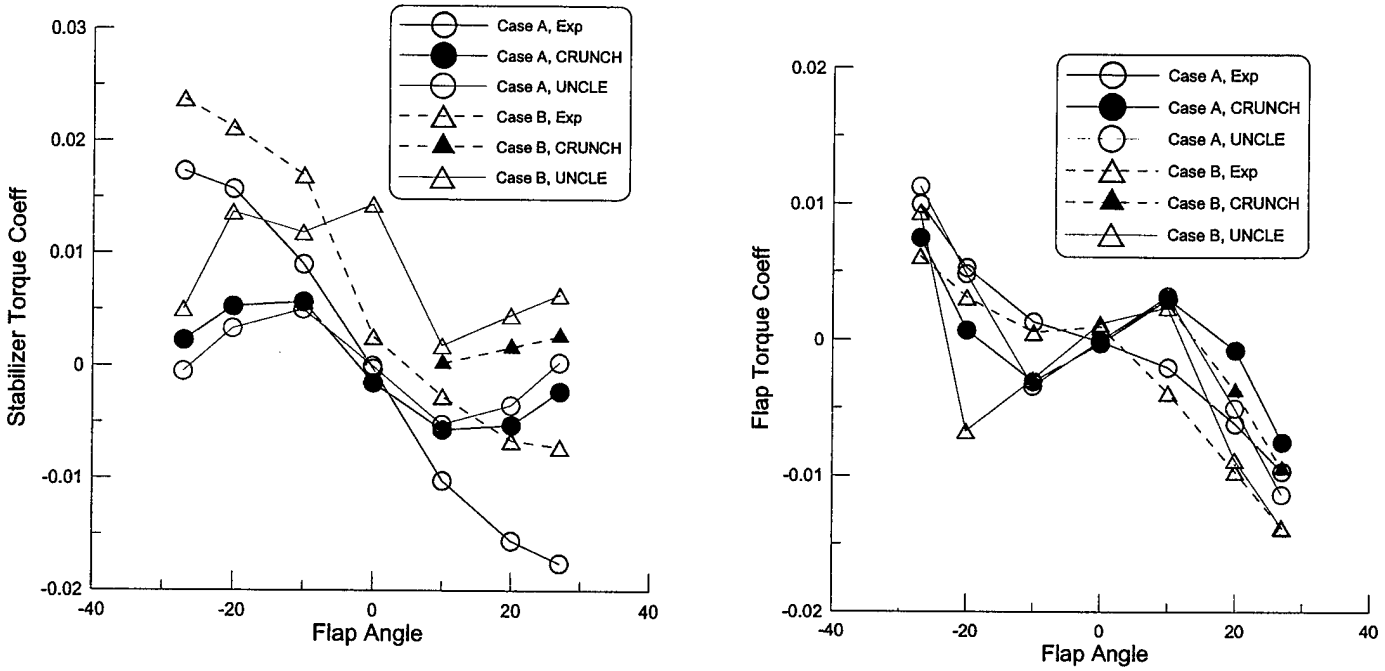

Figure 5. Torque comparisons on stabilizer and flap of the TAC airfoil for Cases A and B.

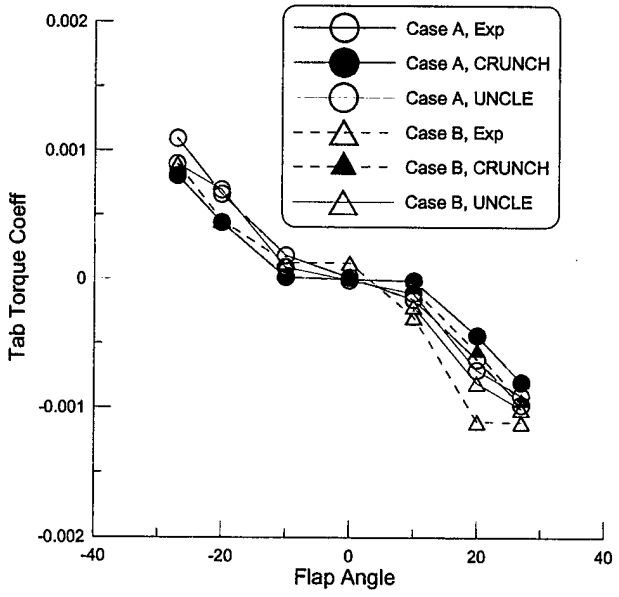

Figure 6. Torque comparisons on tab of the TAC airfoil for Cases A and B.

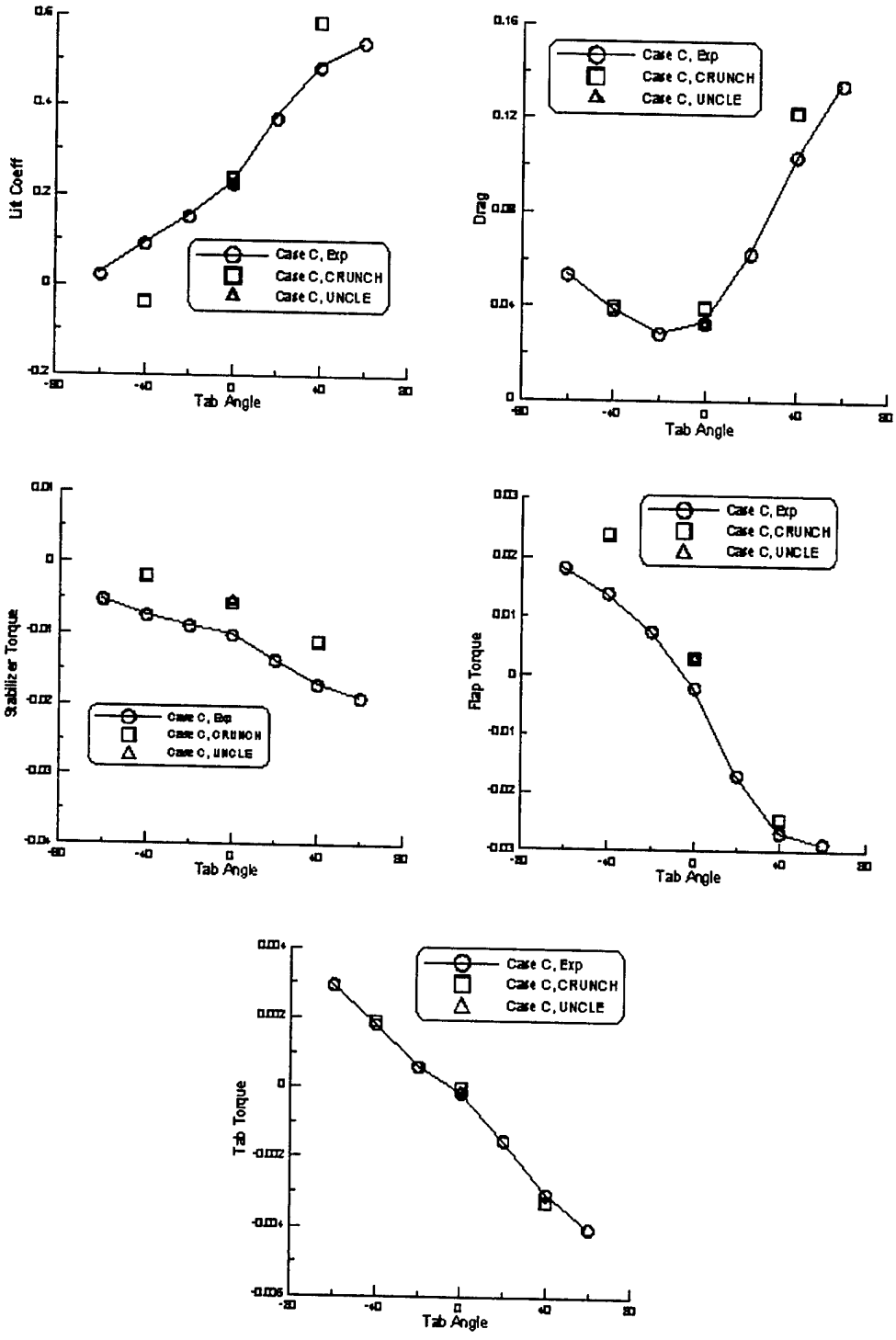

Figure 7. Force and moment comparisons for the TAC airfoil for Case C.

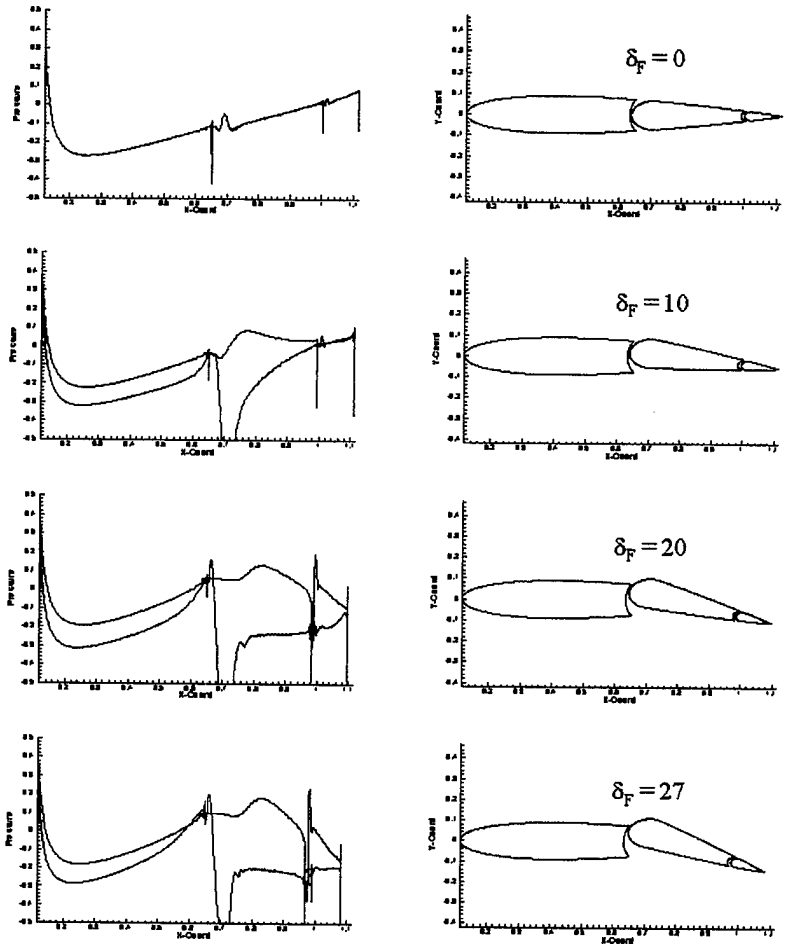

Figure 8. Pressure distributions at mid-span of the TAC foil for Case A.

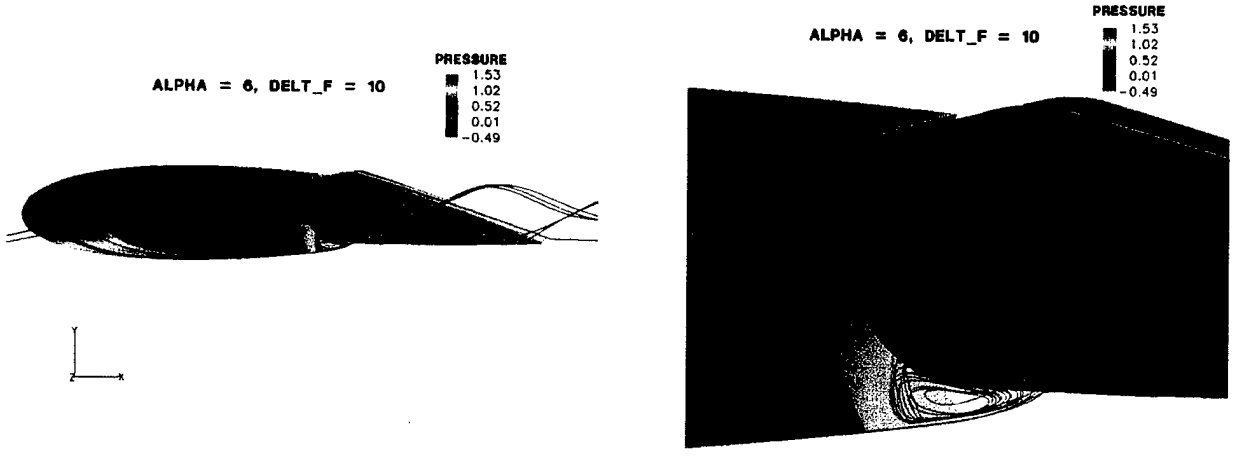

Figure 9. Shedding vortices from the pressure-side trailing corner (color contours represent pressure distribution).

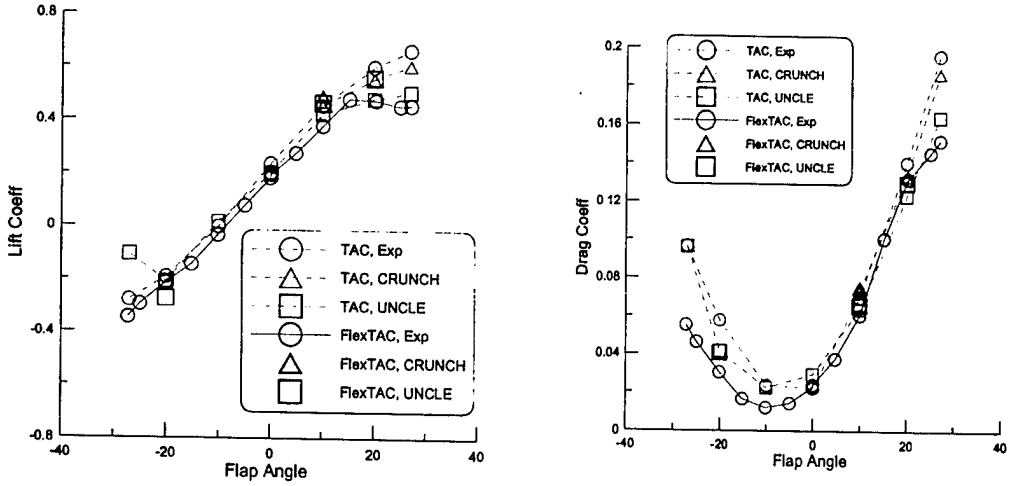

Figure 10. Lift and drag comparisons on TAC and FlexTAC airfoils for Case B.

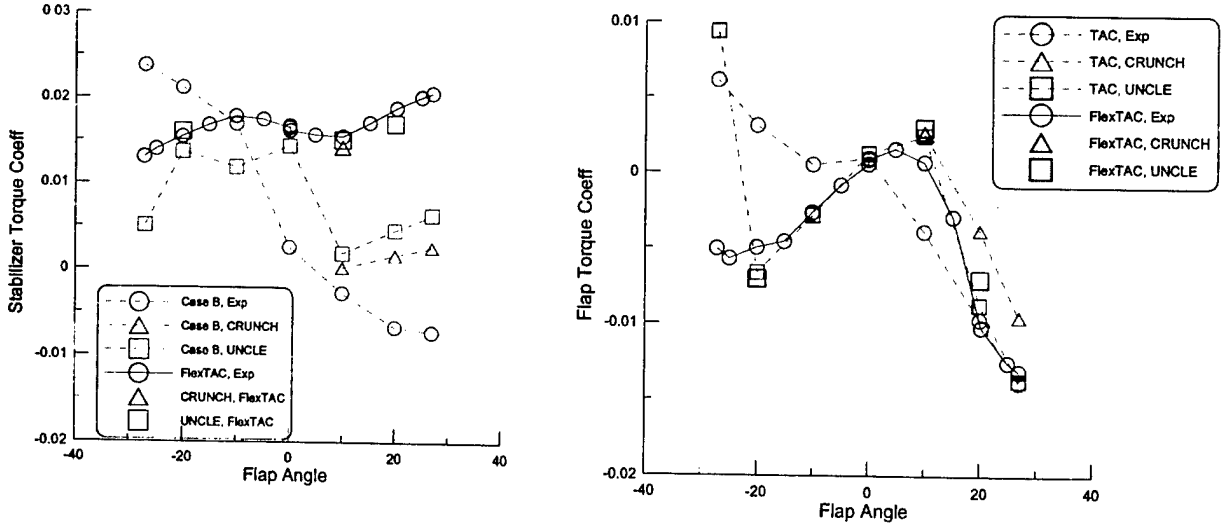

Figure 11. Torque comparisons on TAC and FlexTAC airfoils for Case B.

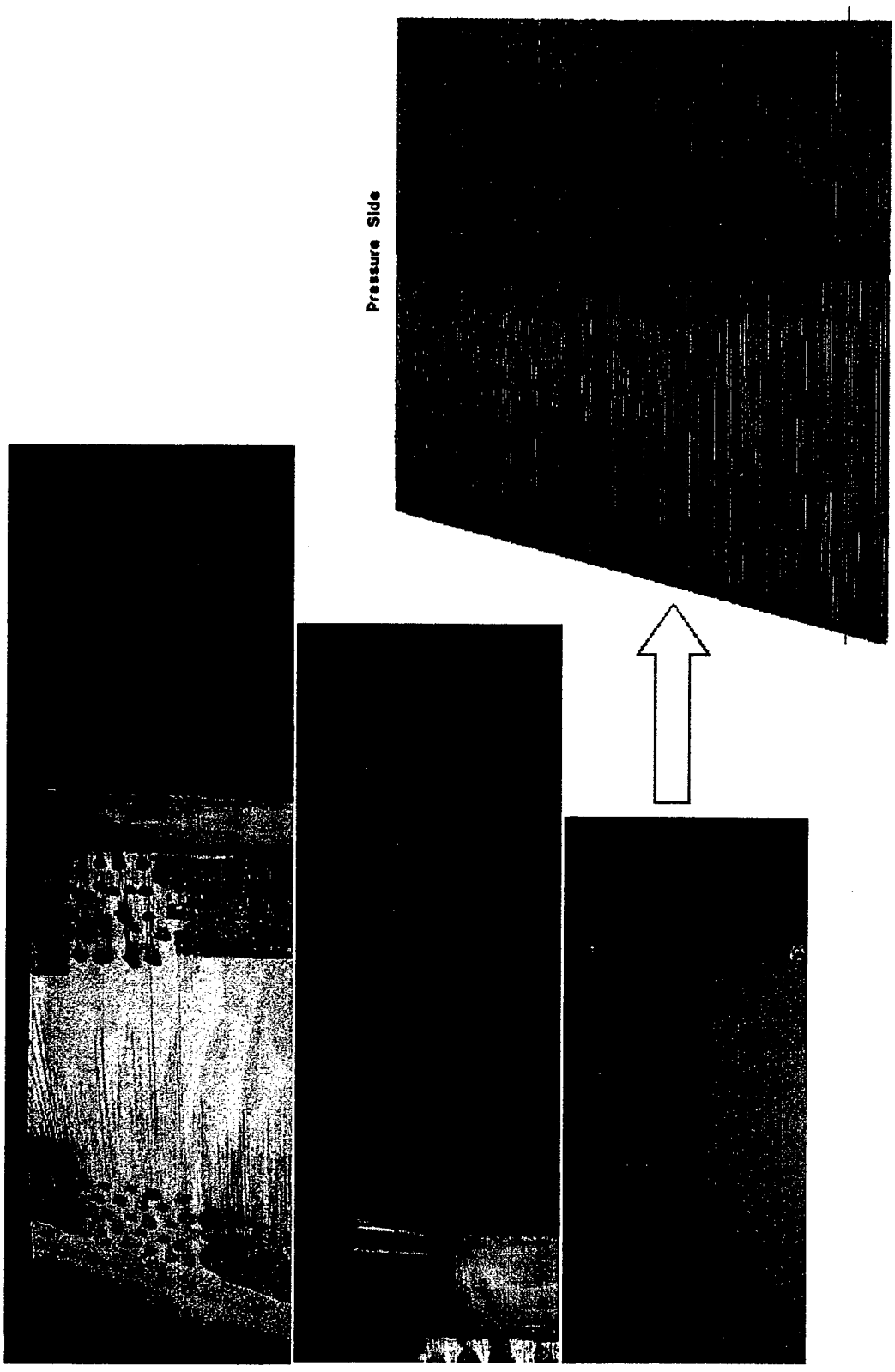

Figure 12. Comparison of paint traces with stremline traces on the pressure side of the FlexTAC airfoil.

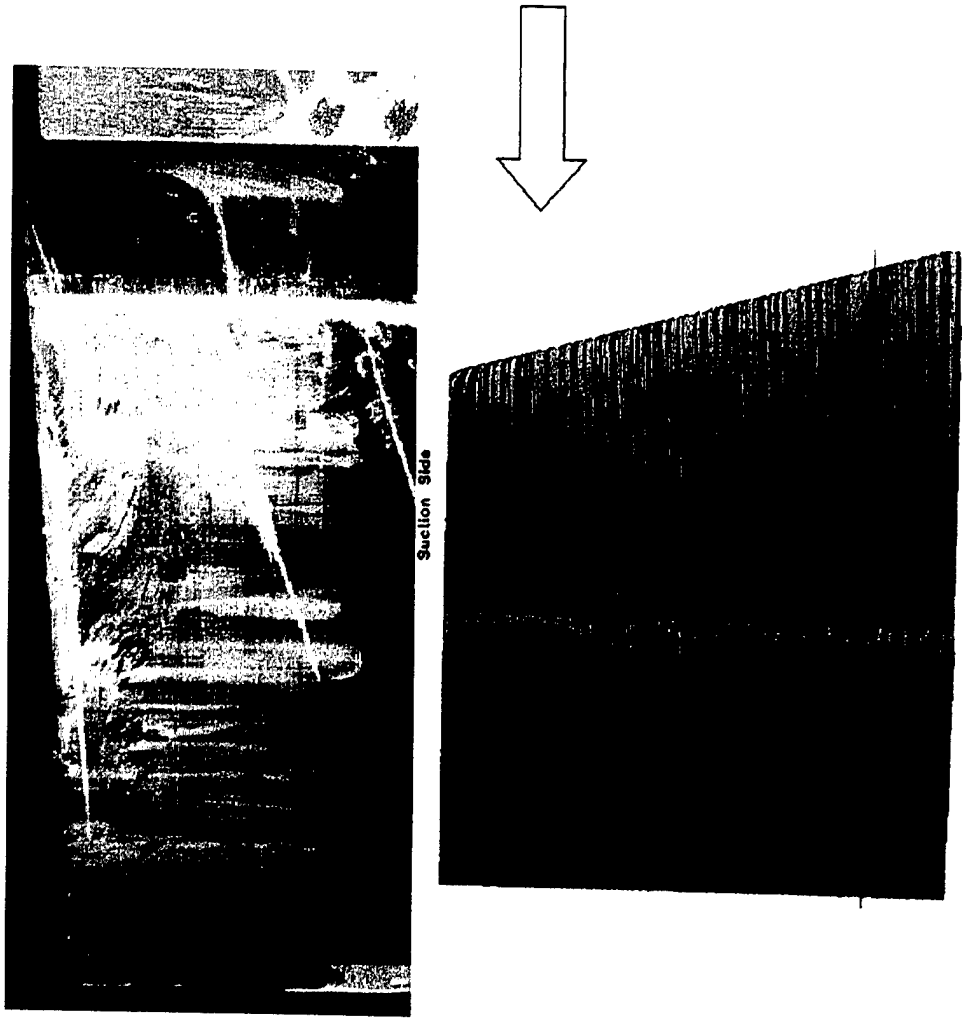

Figure 13. Comparison of paint traces with stremline traces on the suction side of the FlexTAC airfoil.

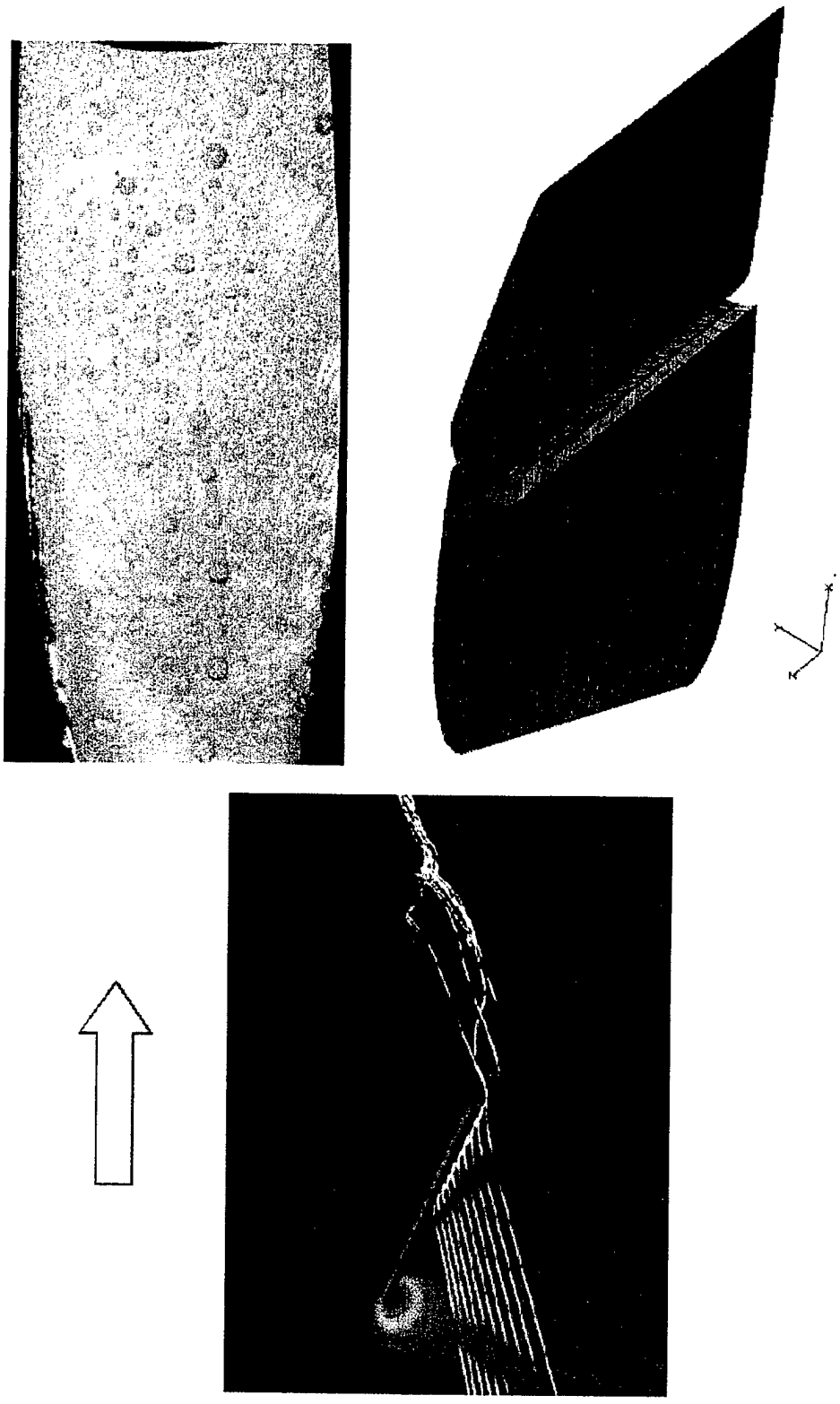

Figure 14. **Comparison of paint traces with stremline traces over the tip of the FlexTAC airfoil.**

THIS PAGE INTENTIONALLY LEFT BLANK

References

Ahuja, V., Hosangadi, A., Arunajatesan, S., (2001) "Simulations of Cavitating Flows Using Hybrid Unstructured Meshes," *J. of Fluids Engineering*, Vol. 123, No. 2, June, pp. 331-340.

Coakley, T. J., Hsieh, T., (1985) "A Comparison between Implicit and Hybrid Methods for the Calculation of Steady and Unsteady Inlet Flows," AIAA Paper 85-1125.

Gaither, J., Marcum, D., Mitchell, B. (2000) "SolidMesh: A Solid Modeling Approach To Unstructured Grid Generation." *7th International Conference on Numerical Grid Generation in Computational Field Simulations.*

Gowing, S., (2002) "Force and Moment Measurements on the FlexTAC Airfoil," NSWCCD 36-inch water-tunnel measurement data, April.

Hosangadi, A., Lee, R. A., York, B. J., Sinha, N., and Dash, S. M., (1996) "Upwind Unstructured Scheme for Three-Dimensional Combusting Flows," *J. of Propulsion and Power*, Vol. 12, No. 3, May-June, pp. 494-503.

Hyams, D. G., Sreenivas, K., Sheng, C., Nichols, S., Taylor, L. K., Briley, W. R., Marcum, D. L., and Whitfield, D. L., (2002) "An Unstructured Multielement Solution Algorithm for Complex Geometry Hydrodynamic Simulations," presented at the 24th Sym. On Naval Hydrodynamics, Fukuoka, Japan, July 8-13.

Lee, Y. T., Luo, L., and Bein, T. W., (2001) "Direct Method for Optimization of a Centrifugal Compressor Vaneless Diffuser," Transactions of the ASME, *J. of Turbomachinery*, Vol. 123, Jan., pp. 73-80.

Marcum, D., and Weatherill, N. (1994) "Unstructured Grid Generation Using Iterative Point Insertion and Local Reconnection" *AIAA*, 33(9):1619-1625.

Nguyen, T. D., Gowing, S., and Bochinski, D., (1999) "Tab-Assisted Control Surface for Marine Application," presented at the International Symposium Warship '99 Naval Submarines 6.

Sung, C. H., and Rhee, B., (1999) "Prediction of Forces and Moments of Rudders with Flap and Tab, Part I. 2D Airfoil with Flap and Tab," presented at the 7th International Conference on Numerical Ship Hydrodynamics, Nantes, France, July 19-22.

Sung, C. H., Rhee, B., and Koh, I.-Y., (2000) "Validation of Tab Assisted Control Surface Computation," presented at the 23rd Sym. On Naval Hydrodynamics, Bassin D'essair Des Carenes, Val De Reuil, France, Sept. 17-22.

THIS PAGE INTENTIONALLY LEFT BLANK

Distribution

	Copies
DOUGLAS J DAHMER SEA93R, 201/3W-421 NAVAL SEA SYSTEMS COMMAND 1333 ISAAC HULL AVENUE S.E. WASHINGTON DC 20376	1
MARGARET C STOUT SEA93R, 201/3W-442 NAVAL SEA SYSTEMS COMMAND 1333 ISAAC HULL AVENUE S.E. WASHINGTON DC 20376	1
CHARLES R CROCKETT SEA5H, 197/2W-1080 NAVAL SEA SYSTEMS COMMAND 1333 ISAAC HULL AVENUE S.E. WASHINGTON DC 20376	1
MATTHEW B KING SEA5H, 197/2W-1090 NAVAL SEA SYSTEMS COMMAND 1333 ISAAC HULL AVENUE S.E. WASHINGTON DC 20376	1
L PATRICK PURTELL CODE 333 BALLSTON CENTRE TOWER ONE 800 NORTH QUINCY ST ARLINGTON VA 22217-5660	1
RONALD D JOSLIN CODE 333 BALLSTON CENTRE TOWER ONE 800 NORTH QUINCY ST ARLINGTON VA 22217-5660	1
KI-HAN KIM CODE 333 BALLSTON CENTRE TOWER ONE 800 NORTH QUINCY ST ARLINGTON VA 22217-5660	1
JEFF HALL ELECTRIC BOAT/GENERAL DYNAMICS 75 EASTERN POINT ROAD GROTON CT 06340	1
BERNIE F CARPENTER B&B CONSULTING 9713 WEST LONG DRIVE LITTLETON CO 80123	1
ASHVIN HOSANGADI CRAFT TECH INC 174 NORTH MAIN STREET BUILDING 3 PO BOX 1150 DUBLIN PA 18917	1

NSWC, CARDEROCK DIVISION INTERNAL DISTRIBUTION

Code	Name	Copies
3442	TIC	5
50		1
5060		1
5400	ANDERSON	1
5400	EBERT	1
5400	GORSKI	1
5400	GOWING	1
5400	Y.T. LEE	5
5600	ABRAMSON	1
5600	AMMEEN	1
5600	HESS	1
5600	KOH	1
5600	LEE	1
5600	MORAN	1
5600	SUNG	1